JACS
JOURNAL OF THE AMERICAN CHEMICAL SOCIETY

Communication

pubs.acs.org/JACS

Impact of Molecular Clustering inside Nanopores on Desorption Processes

Manuel Tsotsalas,[†,‡] Pavel Hejcik,[†] Kenji Sumida,[†] Ziya Kalay,*[,†] Shuhei Furukawa,*[,†,‡] and Susumu Kitagawa*[,†,‡]

[†]Institute for Integrated Cell-Material Sciences (WPI-iCeMS), Kyoto University, Yoshida, Sakyo-ku, Kyoto 606-8501, Japan

[‡]ERATO Kitagawa Integrated Pores Project, Japan Science and Technology Agency, Kyoto Research Park Bldg #3, Shimogyo-ku, Kyoto 600-8815, Japan

Supporting Information

ABSTRACT: Understanding the sorption kinetics of nanoporous systems is crucial for the development and design of novel porous materials for practical applications. Here, using a porous coordination polymer/quartz crystal microbalance (PCP/QCM) hybrid device, we investigate the desorption of various vapor molecules featuring different degrees of intermolecular (hydrogen bonding) or molecule-framework interactions. Our findings reveal that strong intermolecular interactions lead to the desorption process proceeding via an unprecedented metastable state, wherein the guest molecules are clustered within the pores, causing the desorption rate to be temporarily slowed. The results demonstrate the considerable impact of the chemical nature of an adsorbate on the kinetics of desorption, which is also expected to influence the efficiency of certain processes, such as desorption by gas purge.

Among microporous materials, porous coordination polymers (PCPs) have proved important candidates in many industrial and environmental applications, including catalysis, molecular separations and gas storage.[1] To fully exploit the potential of these materials, a detailed knowledge of the adsorption and desorption processes of guest molecules is crucial.[2] In particular, a variety of molecular interactions (guest−guest or guest−framework interactions) can impact the sorption properties, although to date, the optimization of the affinity toward certain targeted guest species has focused on achieving a greater control over the guest−framework interactions. However, the collective dynamics arising from guest−guest interactions is also of importance for practical applications due to their significant impact on not only the adsorption process, but also the desorption (release) of the guest molecules from the pores.[3] Indeed, the latter is a crucial aspect in applications relying on the rapid or controlled evacuation of the molecules accommodated within the framework, although only a few studies have focused in detail on the desorption processes within PCPs.[4] Herein, we show by means of a combined experimental and theoretical study, the impact of intermolecular interactions between adsorbate molecules on the desorption kinetics. The study has revealed that depending on the properties of the guest molecule, the desorption proceeds via a metastable state, at which the release of molecules is temporarily stopped prior to their more complete removal.

Our approach uses an environment-controlled hybrid PCP/QCM system (Figure 1a; QCM: quartz crystal microbalance) allowing the direct observation of small mass changes with a high time resolution throughout the sorption process, allowing the sorption kinetics of various vapor molecules within PCPs to be probed in detail.[5] Note that QCM experiments are typically performed with small sample quantities of just a few micrograms, allowing heat and mass transfer issues that occur with larger sample sizes to be avoided.[6] For this study, we chose the well-known framework $Cu_3(btc)_2$ (Figure 1b; btc^{3-} = 1,3,5-benzenetricarboxylate)[7] as the host framework because the guest−framework interaction has been widely studied both experimentally[8] and theoretically.[9] To investigate the desorption kinetics of chemically different guest molecules, we chose 1-butanol, diethyl ether, and *n*-pentane (Figure 1c−e). These molecules are of a similar size, but are expected to differ

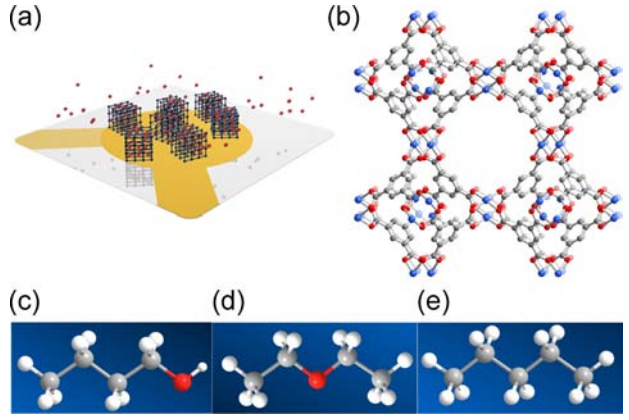

Figure 1. (a) A schematic illustration of the PCP/QCM system where PCP crystals are deposited on a QCM substrate consisting of gold electrodes (yellow) disposed on both sides of a quartz oscillator (transparent plate); (b) a portion of the crystal structure of $Cu_3(btc)_2$; blue, gray, and red spheres represent Cu, C, and O atoms, respectively, H atoms have been omitted for clarity; molecular models of the guest molecules (c) 1-butanol, (d) diethyl ether, and (e) *n*-pentane.

Received: December 12, 2012
Published: March 7, 2013

dx.doi.org/10.1021/ja312115x | *J. Am. Chem. Soc.* 2013, 135, 4608−4611

significantly in their molecule−molecule and molecule−framework interactions. For example, 1-butanol bears an −OH functionality with a propensity to form hydrogen bonds, allowing the effect of strong intermolecular interactions to be studied.[10]

Figure 2a displays the adsorbed normalized mass as a function of time for the guest molecules 1-butanol, diethyl

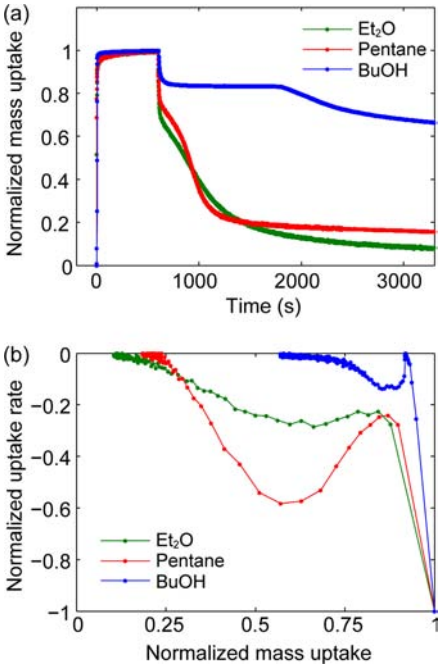

Figure 2. Desorption profiles of 1-butanol, diethyl ether and *n*-pentane from $Cu_3(btc)_2$ as measured using an environment controlled PCP/QCM hybrid device displayed (a) as a function of time, and (b) as a function of normalized mass uptake. Note that the normalized uptake rate is a time derivative of mass uptake obtained by averaging the raw data over 30-s intervals.

ether, and *n*-pentane as measured for relative vapor pressures of 80%. Here, at t = 0, the vapor of the guest molecules is introduced into the helium flow, resulting in a sharp increase in the mass of the substrate due to the adsorption of molecules within the framework until an equilibrium state, in which there is no further mass change over time, is reached. Then, at t = 600 s, the system is purged with helium, which causes the desorption process to begin. In the case of 1-butanol, following a short period in which the mass adsorbed rapidly decreases, desorption temporarily stops before resuming at a later time. The effect is significantly less pronounced for diethyl ether and *n*-pentane, suggesting the phenomenon arises from the chemical nature of the adsorbate. Furthermore, as displayed in Figure 2b, the desorption rate is found to be concentration-dependent.[11] For all guest molecules, the desorption rates fall sharply right after the beginning of the purge process. For diethyl ether and *n*-pentane, this is followed by a period in which the rate of desorption increases temporarily with amount desorbed, and eventually decreases to zero upon removal of most of the adsorbed molecules. However, for 1-butanol, the desorption rate approaches zero shortly after the onset of desorption (after desorption of ∼15% of the 1-butanol molecules), and once the desorption process eventually resumes, the desorption rate increases temporarily and eventually decreases toward zero again. As such, the desorption process proceeds through a bottleneck at a particular concentration of adsorbed guest molecules, leading to a metastable state, during which the desorption rate is effectively zero.

We anticipated the appearance of metastability to be linked with the propensity for 1-butanol molecules to form clusters through intermolecular hydrogen-bonding within the nanopores of $Cu_3(btc)_2$. To further investigate this phenomenon, we studied the sorption kinetics of methanol and ethanol, which form strong hydrogen bonds,[12] as well as molecules featuring much weaker intermolecular interactions (tetrahydrofuran, dichloromethane, hexane and acetone). The desorption profiles of methanol and ethanol also exhibited metastable states similar to that observed for 1-butanol, whereas those for the other molecules did not (Figure S1). The similarity between the desorption profiles of methanol, ethanol, and 1-butanol suggests that strong intermolecular interactions between guest molecules plays a crucial role in the appearance of the metastable state.

As a means for gaining further insight into how the strength of the intermolecular interactions affect the desorption kinetics, we employed a mathematical model of desorption with a concentration-dependent transport diffusion coefficient (see SI for full details). Note that, from the observations of Figure 2 and Figure S1, the transport diffusion coefficient takes a form having a minimum value very close to zero at the guest concentration where the metastable state appears during desorption. As such, in our model, every crystal in the $Cu_3(btc)_2$ sample is considered as an independent unit in which the transport diffusion coefficient strongly depends on the concentration of guest molecules. The desorption profiles resulting from this theoretical model are shown in Figure 3 (see

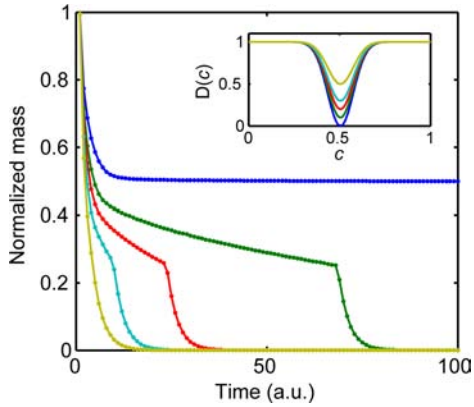

Figure 3. Desorption traces for different intermolecular interaction strengths as calculated by a mathematical model employing a concentration-dependent transport diffusion coefficient. Inset: plots of the transport diffusion coefficient for different intermolecular interaction strengths and a critical concentration of 0.5. In both figures, the only variable parameter is the intermolecular interaction strength ranging from weakest (yellow) to strongest (blue).

inset for a plot of the concentration-dependent diffusion coefficient). Comparing the experimental and theoretical results (see Figures 2a and 3), the simplest model of desorption that ignores details of the internal structure of the PCP can be in qualitative agreement with the observations only when the transport diffusion coefficient is concentration-dependent, such that it has a minimum around a critical value that is associated with the adsorption level at the metastable state.[13]

dx.doi.org/10.1021/ja312115x | J. Am. Chem. Soc. 2013, 135, 4608−4611

To provide a more detailed account on the molecular mechanism behind the metastable state, the pore structure of $Cu_3(btc)_2$ should also be considered. Here, we note that $Cu_3(btc)_2$ has a bimodal pore size distribution consisting of larger cuboctaheral pores with open metal sites on the axial coordination sites of the copper paddlewheel units and smaller, hydrophobic octahedral pores derived from the btc^{3-} units.[7] The effect of this bimodal nature on the sorption properties has been established in previous adsorption studies, in which the sorption isotherms for nitrogen and water exhibited a step feature. Here, the nonpolar nitrogen molecules were first adsorbed in the more confined smaller pores,[14] followed by the larger pores at higher pressures. In contrast, water is accommodated within the larger hydrophilic pores first and then into the smaller hybrophobic pores.[15] The step in the isotherm has been associated with the clustering of guest molecules within the respective pores.[16] Among the adsorption isotherms collected for the molecules investigated by the QCM experiments (Figure S2−S7), the methanol sorption isotherm clearly demonstrates a step at low pressures (Figure S2). From the perspective of its chemical properties, methanol most likely follows a similar adsorption process as water. Moreover, an overlay of the volumetric methanol adsorption isotherm and the desorption kinetic profile as recorded following an adsorption step employing a relative methanol vapor pressure of 10% is shown in Figure 4a. The metastable state observed in the desorption profile and the step in the isotherm appear at the same normalized mass of approximately 0.5, indicating a similar clustering behavior occurring during both adsorption and desorption. In addition, one of the indicators of clustering is the inverse thermodynamic factor defined as:

$$1/\Gamma = (p/c)\cdot(dc/dp) \quad (1)$$

where p is the pressure, c is the concentration of guest molecules, and the $1/\Gamma$ term has been described as the fractional vacancy,[17] which corresponds to the proportion of available adsorption sites. In classic Langmuir adsorption, where there is no clustering, $1/\Gamma$ monotonically decreases from 1 to 0 as adsorption proceeds.[18] However, in the case of clustering, newly introduced molecules can act as adsorption sites themselves, which increases the fractional vacancy to a maximum that could be greater than 1. This maximum value is determined by the spatial constraints imposed by the nanopore environment. Figure 4b illustrates the effect of normalized methanol uptake on the fractional vacancy. Here, in the region of the lower methanol loading, $1/\Gamma$ exceeds unity, which implies that methanol indeed forms clusters in the larger pores before filling up the smaller pores at higher pressures.

To further support the presence of clustering of methanol molecules within the pores of $Cu_3(btc)_2$, infrared spectroscopy was carried out under a controlled vapor pressure of methanol, paying particular attention to the position of the O−H stretching vibration (ν_{O-H}). Note that, for ν_{O-H}, hydrogen bonding induces a significant red-shift (3300−3400 cm^{-1}) and peak broadening compared to free methanol in the gas phase (3700 cm^{-1}).[19] Figure 4c shows the infrared spectra at different relative methanol vapor pressures from 0% to 80%. While no ν_{O-H} absorption was observed in the region from 2000 to 4000 cm^{-1} prior to methanol dosing, characteristically broad peaks at around 3300 cm^{-1} were detected at the lowest pressure of 0.2%. The intensity of this band drastically increased as the pressure was increased to 1.0%, which is a level corresponding to the step in the isotherm. These results indicate the presence

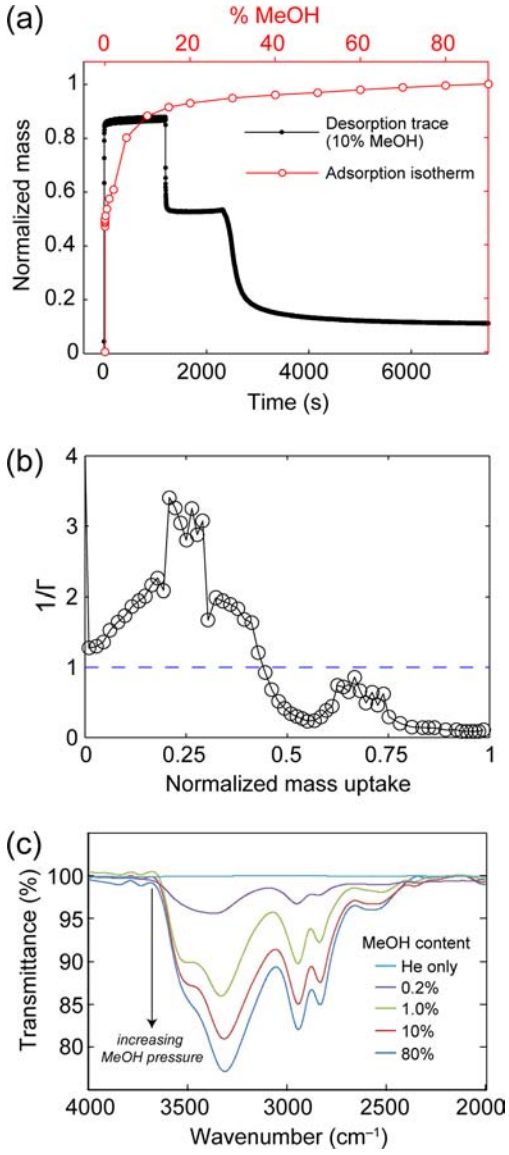

Figure 4. (a) Overlay of the adsorption isotherm of $Cu_3(btc)_2$ for methanol (red) and the kinetic profile of desorption for the 10% vapor pressure of methanol (black); (b) a plot of the inverse thermodynamic factor, $1/\Gamma$, as a function of the normalized mass uptake; (c) infrared transmission spectra of $Cu_3(btc)_2$ under 0%, 0.2%, 1%, 10% and 80% vapor pressure of methanol.

of extensive hydrogen bond formation between methanol molecules in the larger pores.

From these experimental and theoretical results, we can summarize the origin of the metastable state during desorption as follows. When desorption begins, the unclustered molecules in the smaller pores are quickly released due to their relatively low affinity toward the hydrophobic pores. Note that for ZIF-8,[20] which features only hydrophobic pores, the entire amount adsorbed is very rapidly desorbed (see the SI for details). However, the molecules within the larger pores in $Cu_3(btc)_2$ remain due to the formation of clusters through highly interconnected hydrogen bonds among methanol molecules. While the Cu^{2+} adsorption sites on the pore surfaces are expected to be solvated under the conditions of the QCM measurement, the presence of a polar solvent molecule at this site is also expected to contribute to the hydrophilicity of the

dx.doi.org/10.1021/ja312115x | J. Am. Chem. Soc. 2013, 135, 4608−4611

pore surface, and may also provide a site at which the solvent clusters are anchored. The stability of the clusters leads to a period of slow desorption observed as the metastable state, from which molecules are only very slowly desorbed from thermal fluctuations. Eventual disruption of these clusters leads to the resumption of the desorption process.

In conclusion, the present study has demonstrated the impact of collective guest−guest interactions on the desorption processes from nanoporous materials. Further systematic studies aimed at more fully identifying the factors influencing the degree of molecular organization in nanospaces are currently underway using a greater scope of materials and adsorbates, the results of which are expected to afford a greater understanding of the precise structural and chemical properties contributing to the desorption kinetics of nanoporous materials for targeted applications.

■ ASSOCIATED CONTENT

Supporting Information

Experimental details, sorption data, and model description. This material is available free of charge via the Internet at http://pubs.acs.org.

■ AUTHOR INFORMATION

Corresponding Author

zkalay@icems.kyoto-u.ac.jp; shuhei.furukawa@icems.kyoto-u.ac.jp; kitagawa@icems.kyoto-u.ac.jp

Notes

The authors declare no competing financial interest.

■ ACKNOWLEDGMENTS

M.T. and K.S. are grateful to the DAAD and JSPS, respectively, for postdoctoral fellowships. The authors thank Mr. M. Nakahama for experimental assistance. iCeMS is supported by World Premier International Research Initiative (WPI), MEXT, Japan.

■ REFERENCES

(1) (a) Yaghi, O. M.; O'Keeffe, M.; Ockwig, N. W.; Chae, H. K.; Eddaoudi, M.; Kim, J. *Nature* **2003**, *423*, 705. (b) Kitagawa, S.; Kitaura, R.; Noro, S. *Angew. Chem., Int. Ed.* **2004**, *43*, 2334. (c) Ferey, G.; Mellot-Draznieks, C.; Serre, C.; Millange, F. *Acc. Chem. Res.* **2005**, *38*, 217.

(2) (a) Li, J.-R.; Kuppler, R. J.; Zhou, H.-C. *Chem. Soc. Rev.* **2009**, *38*, 1477. (b) Keskin, S.; van Heest, T. M.; Sholl, D. S. *ChemSusChem* **2010**, *3*, 879. (c) Li, J.-R.; Ma, Y.; McCarthy, M. C.; Sculley, J.; Yu, J.; Jeong, H.-K.; Balbuena, P. B.; Zhou, H.-C. *Coord. Chem. Rev.* **2011**, *255*, 1791. (d) Morris, R. E.; Wheatley, P. S. *Angew. Chem., Int. Ed.* **2008**, *47*, 4966. (e) Phan, A.; Doonan, C. J.; Uribe-Romo, F. J.; Knobler, C. B.; O'Keefe, M.; Yaghi, O. M. *Acc. Chem. Res.* **2010**, *43*, 58. (f) Simmons, J. M.; Wu, H.; Zhou, W.; Yildirim, T. *Energy Environ. Sci.* **2011**, *4*, 2177.

(3) (a) Chmelik, C.; Bux, H.; Caro, J.; Heinke, L.; Hibbe, F.; Titze, T.; Karger, J. *Phys. Rev. Lett.* **2010**, *104*, 085902. (b) Grajciar, L.; Bludsky, O.; Nachtigall, P. *J. Phys. Chem. Lett.* **2010**, *1*, 3354. (c) Karra, J. R.; Walton, K. S. *Langmuir* **2008**, *24*, 8620. (d) Munch, A. S.; Mertens, F. O. R. L. *J. Mater. Chem.* **2012**, *22*, 10228. (e) Vaidhyanathan, R.; Iremonger, S. S.; Shimizu, G. K.; Boyd, P. G.; Alavi, S.; Woo, T. K. *Science* **2010**, *330*, 650.

(4) (a) Chmelik, C.; Karger, J. *Chem. Soc. Rev.* **2010**, *39*, 4864. (b) Li, J.-R.; Ma, Y.; McCarthy, M. C.; Sculley, J.; Yu, J.; Jeong, H.-K.; Balbuena, P. B.; Zhou, H.-C. *Coord. Chem. Rev.* **2011**, *255*, 1791.

(5) Uehara, H.; Diring, S.; Furukawa, S.; Kalay, Z.; Tsotsalas, M.; Nakahama, M.; Hirai, K.; Kondo, M.; Sakata, O.; Kitagawa, S. *J. Am. Chem. Soc.* **2011**, *133*, 11932.

(6) Kärger, J.; Ruthven, D. M.; Theodorou, D. N. *Diffusion in Nanoporous Materials*; Wiley-VCH Verlag GmbH & Co. KGaA: Weinheim, 2012; pp 432−433.

(7) Chui, S. S. Y.; Lo, S. M. F.; Charmant, J. P. H.; Orpen, A. G.; Williams, I. D. *Science* **1999**, *283*, 1148.

(8) (a) Wang, Q. M.; Shen, D.; Bülow, M.; Lau, M. L.; Deng, S.; Fitch, F. R.; Lemcoff, N. O.; Semanscin, J. *Microporous Mesoporous Mater.* **2002**, *55*, 217. (b) Bordiga, S.; Regli, L.; Bonino, F.; Groppo, E.; Lamberti, C.; Xiao, B.; Wheatley, P. S.; Morris, R. E.; Zecchina, A. *Phys. Chem. Chem. Phys.* **2007**, *9*, 2676. (c) Panella, B.; Hirscher, M.; Pütter, H.; Müller, U. *Adv. Funct. Mater.* **2006**, *16*, 520. (d) García-Pérez, E.; Gascón, J.; Morales-Flórez, V.; Castillo, J. M.; Kapteijn, F.; Calero, S. *Langmuir* **2009**, *25*, 1725.

(9) (a) Karra, J. R.; Walton, K. S. *Langmuir* **2008**, *24*, 8620. (b) Yang, Q.; Zhong, C. *Chem. Phys. Chem.* **2006**, *7*, 1417. (c) Yang, Q.; Zhong, C. *J. Phys. Chem. B* **2006**, *110*, 17776.

(10) Krishna, R.; van Baten, J. M. *Langmuir* **2010**, *26*, 10854.

(11) Krishna, R.; van Baten, J. M. *Microporous Mesoporous Mater.* **2011**, *138*, 228.

(12) Baber, A. E.; Lawton, T. J.; Sykes, E. C. H. *J. Phys. Chem. C* **2011**, *115*, 9157.

(13) Chmelik, C.; Karger, J.; Wiebcke, M.; Caro, J.; van Baten, J. M.; Krishna, R. *Microporous Mesoporous Mater.* **2009**, *117*, 22.

(14) Krawiec, P.; Kramer, M.; Sabo, M.; Kunschke, R.; Frode, H.; Kaskel, S. *Adv. Eng. Mater.* **2006**, *8*, 293.

(15) Kusgens, P.; Rose, M.; Senkovska, I.; Frode, H.; Henschel, A.; Siegle, S.; Kaskel, S. *Microporous Mesoporous Mater.* **2009**, *120*, 325.

(16) Krishna, R.; van Baten, J. M. *Langmuir* **2010**, *26*, 3981.

(17) Krishna, R.; van Baten, J. M. *Microporous Mesoporous Mater.* **2011**, *142*, 745.

(18) Krishna, R.; van Baten, J. M. *Langmuir* **2010**, *26*, 3981.

(19) Schenkel, R.; Jentys, A.; Parker, S. F.; Lercher, J. A. *J. Phys. Chem. B* **2004**, *108*, 15013.

(20) Huang, X. C.; Lin, Y. Y.; Zhang, J. P.; Chen, X. M. *Angew. Chem., Int. Ed.* **2006**, *45*, 1557.